J Geod (2017) 91:25–40
DOI 10.1007/s00190-016-0935-4

ORIGINAL ARTICLE

Ambiguity resolved precise point positioning with GPS and BeiDou

Li Pan[1,2] · **Zhang Xiaohong**[1,2,3] · **Guo Fei**[1,2,3]

Received: 29 September 2015 / Accepted: 27 June 2016 / Published online: 9 July 2016

Abstract This paper focuses on the contribution of the global positioning system (GPS) and BeiDou navigation satellite system (BDS) observations to precise point positioning (PPP) ambiguity resolution (AR). A GPS + BDS fractional cycle bias (FCB) estimation method and a PPP AR model were developed using integrated GPS and BDS observations. For FCB estimation, the GPS + BDS combined PPP float solutions of the globally distributed IGS MGEX were first performed. When integrating GPS observations, the BDS ambiguities can be precisely estimated with less than four tracked BDS satellites. The FCBs of both GPS and BDS satellites can then be estimated from these precise ambiguities. For the GPS + BDS combined AR, one GPS and one BDS IGSO or MEO satellite were first chosen as the reference satellite for GPS and BDS, respectively, to form inner-system single-differenced ambiguities. The single-differenced GPS and BDS ambiguities were then fused by partial ambiguity resolution to increase the possibility of fixing a subset of decorrelated ambiguities with high confidence. To verify the correctness of the FCB estimation and the effectiveness of the GPS + BDS PPP AR, data recorded from about 75 IGS MGEX stations during the period of DOY 123-151 (May 3 to May 31) in 2015 were used for validation. Data were processed with three strategies: BDS-only AR, GPS-only AR and GPS + BDS AR. Numerous experimental results show that the time to first fix (TTFF) is longer than 6 h for the BDS AR in general and that the fixing rate is usually less than 35 % for both static and kinematic PPP. An average TTFF of 21.7 min and 33.6 min together with a fixing rate of 98.6 and 97.0 % in static and kinematic PPP, respectively, can be achieved for GPS-only ambiguity fixing. For the combined GPS + BDS AR, the average TTFF can be shortened to 16.9 min and 24.6 min and the fixing rate can be increased to 99.5 and 99.0 % in static and kinematic PPP, respectively. Results also show that GPS + BDS PPP AR outperforms single-system PPP AR in terms of convergence time and position accuracy.

Keywords Precise point positioning · Ambiguity resolution · Time to first fix · Combined GPS and BDS · Fixing rate · Fractional cycle bias

✉ Zhang Xiaohong
xhzhang@sgg.whu.edu.cn

[1] School of Geodesy and Geomatics, Wuhan University, 129 Luoyu Road, Wuhan 430079, China

[2] Key Laboratory of Geospace Environment and Geodesy, Ministry of Education, 129 Luoyu Road, Wuhan 430079, China

[3] Collaborative Innovation Center for Geospatial Technology, 129 Luoyu Road, Wuhan 430079, China

1 Introduction

Precise point positioning (PPP) (Zumberge et al. 1997; Kouba and Héroux 2001) is a single-receiver positioning technique that enables global centimetre-level positioning accuracy. PPP is a powerful and efficient tool and has been widely used for scientific and civilian applications. In recent years, to improve PPP positioning accuracy as well as its convergence, ambiguity resolution (AR) techniques relying only on a single receiver has aroused interest amongst the scientific community. A wide range of studies has been conducted concerning the fractional cycle bias (FCB) estimation, AR method, performance and scientific applications (Ge et al. 2008; Collins et al. 2008; Laurichesse et al. 2009; Loyer et al. 2012; Li and Zhang 2014, 2015; Geng et al. 2009).

Ge et al. (2008) developed a method to estimate the FCB by averaging the fractional parts of the float wide-lane (WL) and narrow-lane (NL) ambiguity estimates. Once the single-

differenced ambiguities between satellites are fixed, PPP accuracy can be improved significantly, especially in the easting component. Since January 1, 2015, the School of Geodesy and Geomatics at Wuhan University (SGG-WHU) routinely releases the WL and NL GPS FCB products, based on a modified version of Ge's FCB estimation method, with open access (Li et al. 2015a). Collins et al. (2008) also developed a method known as the decoupled clock model that is characterized by separated satellite clocks for code and phase observations and can be used for separating receiver/satellite code/phase biases from PPP ambiguities. Similarly, Laurichesse et al. (2009) developed an integer phase clock model in which the NL FCBs were assimilated into receiver and satellite clock estimates of a GPS network solution. This model has been employed to generate the Groupe de Recherche de Géodésie Spatiale (GRGS) precise satellite clock by the Centre National d'Etudes Spatiales (CNES) (Loyer et al. 2012) to absorb the integer-recovered clock corrections. These various FCB methods are distinguished by the attributes of the integer satellite product used and, in theory, have been demonstrated to be equivalent to each other (Geng et al. 2010).

In addition, studies to improve the GPS PPP AR model and strategy have also been conducted by many researchers. Li and Zhang (2015) proposed a partial AR (PAR) method for GPS PPP. They achieved a much higher fixing rate with this method and quicker convergence to the first fixed solution compared with the PPP results with full AR (FAR). More studies on PPP PAR can be found in Huber et al. (2014), Shi and Gao (2012) and Verhagen et al. (2011). Li et al. (2013) presented a PPP AR model that was different from the conventional ionosphere-free (IF) combination model; their model was based on the raw GPS L1 and L2 observations, with the empirical spatial and temporal constraints and a priori ionospheric model all considered as pseudo-observations for the estimation of the ionosphere parameters. Their results indicated that the time for ambiguity-fixing was shortened by 25 % compared to that of the traditional ambiguity-fixed kinematic solution. Moreover, Geng and Bock (2013) proposed a method where the simulated triple-frequency GPS signals were exploited to enable rapid convergence to ambiguity-fixed solutions in real-time PPP. The extra-wide-lane (EWL), WL ambiguities derived from an IF observable with a wavelength of approximately 3.4 m and the NL ambiguities were fixed sequentially. Based on a method with simulated triple-frequency GPS signals, their results showed that the correctness rate of NL AR achieved 99 % within 65 s, in contrast to only 64 % within 150 s in dual-frequency PPP.

The studies mentioned above were conducted with GPS-only systems. GLONASS is another satellite system that has reached full operational capability with global coverage since 2011. However, because there are frequency/receiver type-specific inter-frequency biases in the GLONASS pseudorange and carrier phase measurements (Reussner and Wanninger 2011; Sleewaegen et al. 2012) caused by the frequency-division multiple access technique of the GLONASS signals, fixing GLONASS PPP ambiguity is still considered to be difficult. Jokinen et al. (2013) studied the impact of adding GLONASS observations to GPS ambiguity-fixed PPP on the time to first fix (TTFF) which is defined as the time taken for the ambiguity terms to be first successfully fixed (Feng and Wang 2008; Gao et al. 2015). They assigned a much smaller weight to both the GLONASS code and phase observations. The results showed that the inclusion of GLONASS can reduce the TTFF by approximately 5 % compared to employing GPS alone. Li and Zhang (2014) also investigated the performance of GPS PPP AR with GPS+GLONASS combined PPP. Their results showed that the average TTFF of GPS AR can be reduced by 27.4 and 42.0 % in static and kinematic modes, respectively, with the aid of the GLONASS observations. Moreover, the less the GPS satellites were used in float PPP, the more significant the reduction in TTFF was when adding GLONASS observations. Similar results on GLONASS-aided GPS PPP AR have been reported in Pan et al. (2014).

In addition to GPS and GLONASS, the Chinese BeiDou system (BDS) launched a regional navigation service in 2012 and has continued development toward a global system in the near future (http://en.beidou.gov.cn/). Currently, (November 1, 2015), C13 is no longer working, and the observations from satellites launched in 2015 are still not available; a total of 13 BDS satellites have been in operation, including five geostationary orbits (GEO), five inclined geosynchronous orbits (IGSO) and three medium altitude Earth orbits (MEO). Based on the data and products generated with the IGS Multi-GNSS Global Experiment (MGEX) (Steigenberger et al. 2013), BDS has demonstrated its independent potential for both relative positioning and PPP throughout the Asia-Pacific region (Li et al. 2014; Teunissen et al. 2014). Qu et al. (2015) demonstrated preliminary results of ambiguity-fixed PPP with BDS-only and combined BDS+GPS by using only one-day multi-GNSS data. Gu et al. (2015) conducted triple-frequency ambiguity-fixed PPP based on real tracking BDS data. The EWL and WL ambiguity subsets were manually formed based on the raw ambiguity estimates and were then fixed with integer least-squares, whereas the BDS L1 ambiguities were kept as float values. Based on two experiments with a typical inter-station distance of 400 and 800 km, it was shown that the EWL and WL AR can obviously improve the PPP in terms of both precision and convergence.

Based on the above reviews, we conclude that most existing work mainly focuses on fixing the GPS PPP ambiguity. Only the initial results of the BDS PPP AR with regional GNSS data have been given by Qu et al. (2015) and Gu et al. (2015). How to realize a reliable dual-system PPP AR with

fully integrated GPS and BDS observations and what can be achieved in terms of AR performance with respect to TTFF and fixing rate are still not clear. Additionally, how to estimate precise BDS FCB products is another important issue of concern for combined GPS and BDS PPP AR. The BDS FCBs are expected to be estimated using the globally distributed BDS data, such as the observations from MGEX. Furthermore, the BDS FCBs are expected to better serve the worldwide application of BDS-related PPP AR.

In this study, we propose a GPS + BDS FCB estimation method based on the combined PPP model to realize the GPS + BDS PPP AR. A PAR strategy is employed to fix the single-differenced GPS and BDS ambiguities to increase the possibility of fixing partial ambiguities with high confidence when FAR fails. The performance of the GPS + BDS combined PPP AR is also investigated and compared to that of PPP AR with a single-system. The advantages of combined PPP data processing over single-system processing for FCB estimation and PPP AR are fully discussed. This paper is organized as follows: Sect. 2 formulates the combination observables, addresses the methods applied to GPS + BDS FCB estimation and evaluates the quality of GPS and BDS FCBs; Sect. 3 describes the PPP AR processing strategy and experiment scenarios; Sect. 4 analyses the performance of combined PPP AR in terms of TTFF and the fixing rate and compares the results of combined PPP AR with those of single-system PPP AR solutions. Finally, Sect. 5 presents the conclusions and perspectives.

2 Network processing

We start with the basic GPS and BDS observational equations and then give a detailed description of our FCB estimation and PPP AR method.

2.1 GPS and BDS observation equations

To eliminate the first-order ionospheric delays in the pseudorange and carrier-phase measurements, IF combination observations are normally used by the IGS analysis centre to produce a precise satellite clock and orbit. These combinations are also used by the PPP software to estimate the parameters of interest. For a satellite s (GPS denoted by 'G' and BDS denoted by 'C') observed by receiver r, the IF combination of pseudorange P and carrier phase L observations can be expressed as

$$P_{\mathrm{r,IF}}^{\mathrm{s,G}} = \rho_{\mathrm{r}}^{\mathrm{s,G}} + c(\mathrm{d}t_{\mathrm{r}}^{\mathrm{G}} - \mathrm{d}t^{\mathrm{s,G}}) + T_{\mathrm{r}}^{\mathrm{s,G}} + b_{\mathrm{r,IF}}^{G} - b_{\mathrm{IF}}^{\mathrm{s,G}} + e_{\mathrm{r,IF}}^{\mathrm{s,G}} \tag{1}$$

$$L_{\mathrm{r,IF}}^{\mathrm{s,G}} = \rho_{\mathrm{r}}^{\mathrm{s,G}} + c(\mathrm{d}t_{\mathrm{r}}^{\mathrm{G}} - \mathrm{d}t^{\mathrm{s,G}}) + T_{\mathrm{r}}^{\mathrm{s,G}} + \lambda_{\mathrm{IF}}^{\mathrm{G}} \cdot (N_{\mathrm{r,IF}}^{\mathrm{s,G}} + B_{\mathrm{r,IF}}^{\mathrm{G}} - B_{\mathrm{IF}}^{\mathrm{s,G}}) + \varepsilon_{\mathrm{r,IF}}^{\mathrm{s,G}} \tag{2}$$

$$P_{\mathrm{r,IF}}^{\mathrm{s,C}} = \rho_{\mathrm{r}}^{\mathrm{s,C}} + c(\mathrm{d}t_{\mathrm{r}}^{\mathrm{C}} - \mathrm{d}t^{\mathrm{s,C}}) + T_{\mathrm{r}}^{\mathrm{s,C}} + b_{\mathrm{r,IF}}^{\mathrm{C}} - b_{\mathrm{IF}}^{\mathrm{s,C}} + e_{\mathrm{r,IF}}^{\mathrm{s,C}} \tag{3}$$

$$L_{\mathrm{r,IF}}^{\mathrm{s,C}} = \rho_{\mathrm{r}}^{\mathrm{s,C}} + c(\mathrm{d}t_{\mathrm{r}}^{\mathrm{C}} - \mathrm{d}t^{\mathrm{s,C}}) + T_{\mathrm{r}}^{\mathrm{s,C}} + \lambda_{\mathrm{IF}}^{\mathrm{C}} \cdot (N_{\mathrm{r,IF}}^{\mathrm{s,C}} + B_{\mathrm{r,IF}}^{\mathrm{C}} - B_{\mathrm{IF}}^{\mathrm{s,C}}) + \varepsilon_{\mathrm{r,IF}}^{\mathrm{s,C}}, \tag{4}$$

where ρ is the geometric distance, c is the speed of light, $\mathrm{d}t_{\mathrm{r}}$ and $\mathrm{d}t^{\mathrm{s}}$ are the clock errors of receiver and satellite, respectively; $T_{\mathrm{r}}^{\mathrm{s}}$ is the slant troposphere delay; $b_{\mathrm{r,IF}}$ is the code hardware delay from receiver antenna to the signal correlator in the receiver; $b_{\mathrm{IF}}^{\mathrm{s}}$ is the code hardware delay from the satellite signal generator to the satellite antenna; e is the pseudorange measurement noise; λ_{IF} is the wavelength of the IF carrier phase; $N_{\mathrm{r,IF}}^{\mathrm{s}}$ is the carrier phase ambiguity; $B_{\mathrm{r,IF}}$ and $B_{\mathrm{IF}}^{\mathrm{s}}$ are the IF receiver-dependent and satellite-dependent carrier phase hardware delay, respectively; and ε is the measurement noise of the carrier phase. Other error items, such as the phase centre offset (PCO) and variation (PCV) (Schmid et al. 2005), phase wind-up (Wu et al. 1993), relativistic effect, tide loading and so on, are assumed to be precisely corrected with their corresponding models (Petit and Luzum 2010).

For GNSS observations, the pseudorange IF hardware delay biases at the satellite side $b_{\mathrm{IF}}^{\mathrm{s}}$ are assimilated into the clock offset $c \cdot \mathrm{d}t^{\mathrm{s}}$ following the IGS analysis convention. Because the pseudorange observation provides a reference to the clock parameters, the actual receiver clock estimate would absorb the IF combination of the receiver hardware delay $b_{\mathrm{r,IF}}$ in the PPP software under the assumption that the receiver hardware delay will be the same for satellites from the same constellation for the same spectral band (Chen et al. 2015; Guo et al. 2015). Therefore, after applying GPS + BDS precise satellite clocks, the re-parameterized ambiguities read as (for the sake of simplicity, the symbol denoting the satellite system is not given)

$$\bar{N}_{\mathrm{r,IF}}^{\mathrm{s}} = N_{\mathrm{r,IF}}^{\mathrm{s}} + d_{\mathrm{r,IF}} - d_{\mathrm{IF}}^{\mathrm{s}} \tag{5}$$

$$d_{\mathrm{r,IF}} = B_{\mathrm{r,IF}} - b_{\mathrm{r,IF}}/\lambda_{\mathrm{IF}} \tag{6}$$

$$d_{\mathrm{IF}}^{\mathrm{s}} = B_{\mathrm{IF}}^{\mathrm{s}} - b_{\mathrm{IF}}^{\mathrm{s}}/\lambda_{\mathrm{IF}}, \tag{7}$$

where $d_{\mathrm{r,IF}}$ is the linear combination of IF pseudorange and carrier phase hardware delay at receiver side, while $d_{\mathrm{IF}}^{\mathrm{s}}$ is the linear combination of IF pseudorange and carrier phase hardware delay at satellite side.

The tropospheric delay is split into a hydrostatic (dry) part and a non-hydrostatic (wet) part. The zenith dry component of tropospheric delays can be corrected with the Saastamoinen model (1972). The zenith wet delay (ZWD) should be estimated as an unknown. The global mapping functions (Boehm et al. 2006) can be used to project the slant dry and wet delays to the zenith delays. Additionally, the troposphere gradient parameters are estimated in our software

to account for the bulk of the asymmetric delay. The clock parameter is normally treated as an epoch-wise parameter for a single-system PPP. For the combined GPS + BDS PPP, a GPS receiver clock and an inter-system time difference parameter (known as ISB) is estimated. $d_{r,IF}$ and d^s_{IF} are linearly dependent on the ambiguity and are considered to be stable over time. Thus, they are grouped into the ambiguity in ambiguity-float data processing (Chen et al. 2015). For an ambiguity-float PPP solution, the ambiguity parameter $\bar{N}^s_{r,IF}$ is estimated as a real-value constant. For an ambiguity-fixed PPP solution $\bar{N}^s_{r,IF}$ is usually decomposed into the combination of integer WL and float NL ambiguities because the L1 and L2 ambiguities cannot be estimated simultaneously in an IF PPP (Dach et al. 2007),

$$\bar{N}^s_{r,IF} = \left(\frac{c \cdot f_2}{f_1^2 - f_2^2} N^s_{r,WL} + \frac{c}{f_1 + f_2} \bar{N}^s_{r,NL} \right) \Big/ \lambda_{IF} \tag{8}$$

with

$$\bar{N}^s_{r,WL} = N^s_{r,WL} + d_{r,WL} - d^s_{WL} \tag{9}$$

$$\bar{N}^s_{r,NL} = N^s_{r,NL} + d_{r,NL} - d^s_{NL}, \tag{10}$$

where f_1 and f_2 are the carrier frequency of L1 and L2, respectively; $N^s_{r,WL}$ is the WL integer ambiguity and $\bar{N}^s_{r,WL}$ is the WL float ambiguity which can be calculated with the Melbourne–Wübbena (MW) combination observable (Melbourne 1985; Wubbena 1985); $\bar{N}^s_{r,NL}$ is the derived NL float ambiguity and $N^s_{r,NL}$ is the NL integer ambiguity; $d_{r,WL}$ and d^s_{WL} are the undifferenced WL FCB at receiver and satellite side, respectively; $d_{r,NL}$ and d^s_{NL} are the undifferenced NL FCB at receiver and satellite side, respectively.

2.2 FCB estimation for GPS and BDS

The FCB estimation method proposed by Ge et al. (2008) is modified and then applied to generate the GPS and BDS WL and NL FCB products. The undifferenced WL and NL ambiguity estimates, which are derived from the MW combination and the real-valued IF ambiguities can be further formulated as (Loyer et al. 2012)

$$R^s_r \equiv \bar{N}^s_r - N^s_r = d_r - d^s, \tag{11}$$

where R^s_r is the combined fractional part of FCBs from both receiver r and satellite s, $\bar{N}^s_r$ denotes float undifferenced ambiguities of the PPP, N^s_r denotes the integer part of $\bar{N}^s_r$, and d_r and d^s denote receiver and satellite FCBs, respectively.

A set of equations in the form of (11) can be formed with the estimated ambiguities from a reference network. The equations will have a rank defect of 1 because of the linear dependence between d_r and d^s. For our estimation, the rank defect is eliminated by introducing an extra constraint of fixing one of the satellite FCBs to zero (Zhang and Li 2013). The FCB products of other satellites referenced to that satellite can then be estimated by least-squares. The healthy satellite with the maximum number of observations would be selected as the reference. Each input ambiguity would be weighted according to its variance. The variance of the WL ambiguity is that of the MW combinations in a continuous arc, whereas the variance of the NL ambiguity is propagated from that of the IF ambiguity (Ge et al. 2008).

As reported by Wanninger and Beer (2015), BDS, as opposed to GPS, is unfortunately subjected to satellite-induced pseudorange variations, which are elevation and frequency dependent while time and azimuth independent. Such code bias variations reach over 1 m for BDS IGSOs and MEOs. They severely affect the precision and stability of the WL ambiguity from the MW combination and finally degrade the quality of BDS WL FCB. Additionally, the precision of BDS PPP ambiguity estimations would be degraded by these code bias variations because the biased pseudorange observations contribute to the parameter estimation. In their study, a correction model was developed and the correction parameters were determined for BDS IGSO and MEO satellites. Their correction parameters have been successfully used in single-frequency BDS PPP to eliminate the systematic bias in height component and improve the position accuracy. Therefore, their code bias corrections are used in this study to mitigate the effect of these code biases on BDS FCB estimation and PPP AR. It should be noted that the FCBs of the BDS GEO satellites are not yet estimated and that the BDS GEO ambiguity parameter is not fixed for ambiguity-fixed PPP in this paper because of the poor orbit quality of the GEO satellites as well as the insufficient solar radiation pressure models used in the current constellation (Li et al. 2015b; Lou et al. 2014; Zhao et al. 2013). However, the measurements of the BDS GEO satellites are used for ambiguity-float PPP data processing. In the interest of brevity, "BDS FCB" denotes "FCB of BDS IGSO and MEO satellites", and "BDS AR" denotes "AR with the ambiguities of BDS IGSO and MEO satellites".

The GPS + BDS observations from the reference network shown in Fig. 1 are processed in dual-system PPP model to generate WL and IF ambiguities for FCB estimation. To give a visual presentation of the geometry strength with different satellite constellations, Fig. 2 shows the global distribution of the number of visible single- and dual- system satellites, with an elevation cut-off of 15°, at GPS time 2015/05/10 00:00:00.0. As shown in Fig. 2, BDS has a better coverage in the Asia-Pacific area. However, the number of available BDS IGSO and MEO satellites is still quite limited (usually less than 7). The situation is even worse in other regions.

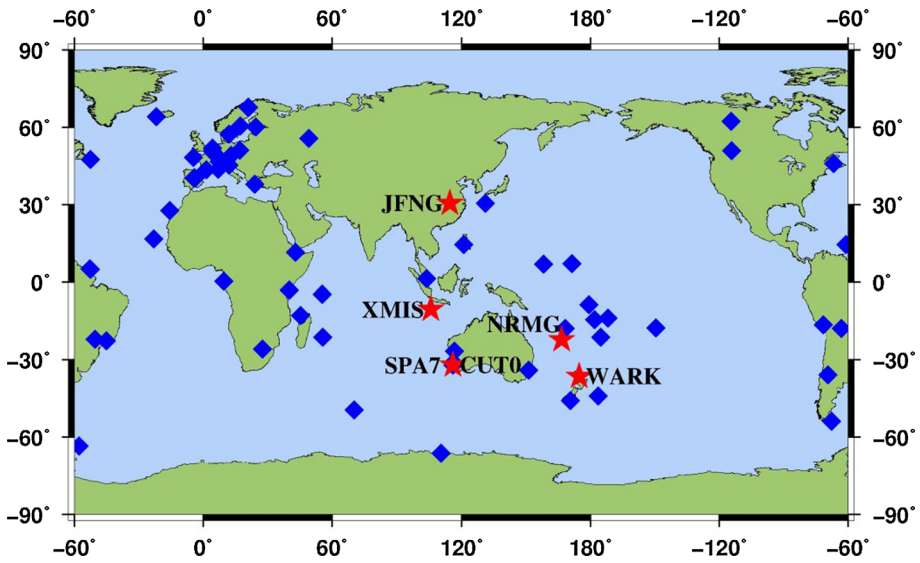

Fig. 1 Distribution of the GPS + BDS reference network and user stations. The *blue diamonds* denote the reference stations used for FCB estimations; the *red stars* denote the user stations used for investigating the performance of the single- and dual- system PPP ARs. The distance between CUT0 and SPA7 is less than 500 m, causing the *star symbols* of these two stations to almost overlap

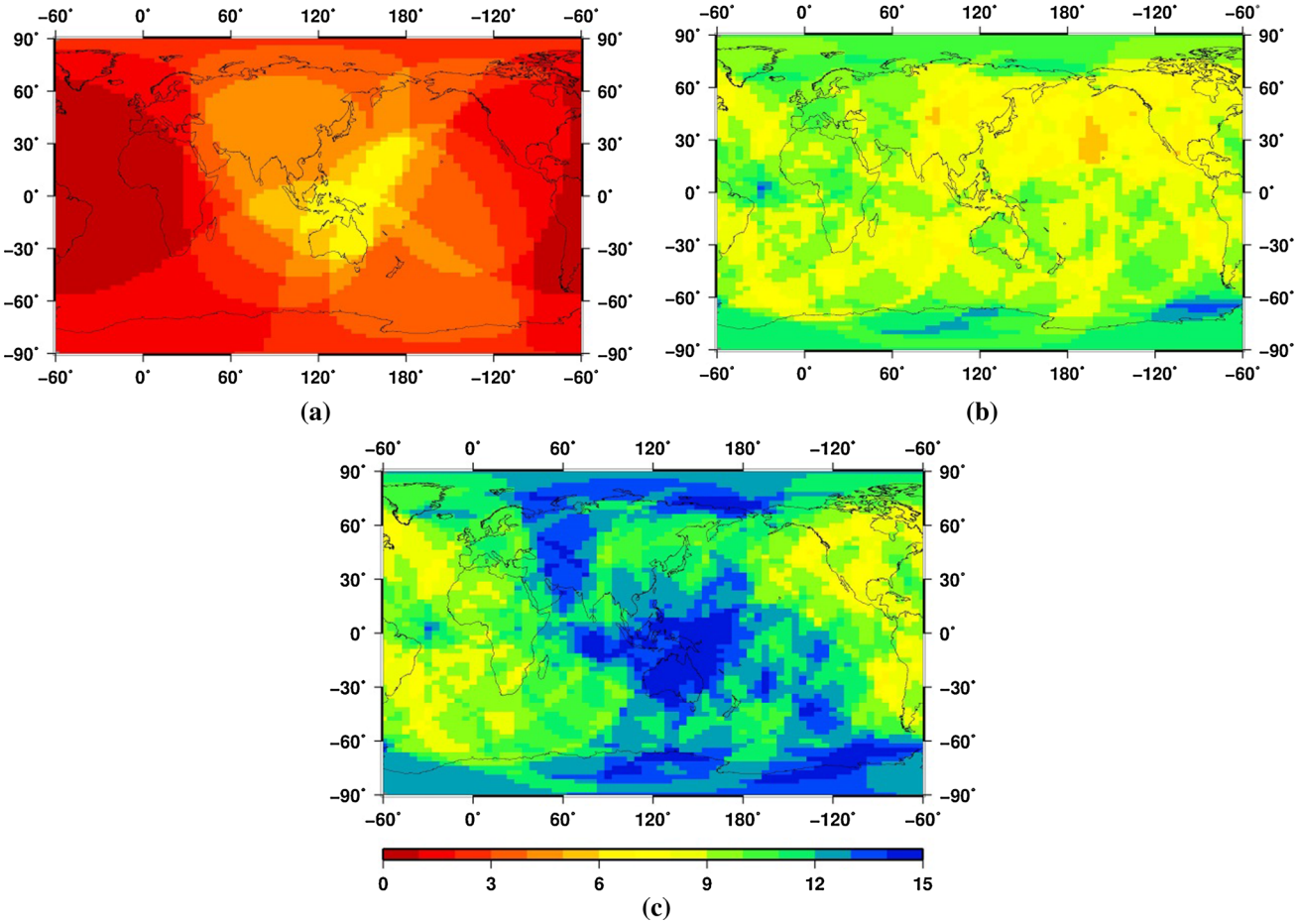

Fig. 2 Distribution of the number of visible BDS IGSO and MEO (**a**), GPS (**b**), GPS and BDS IGEO + MEO (**c**) at epoch 2015/05/10 00:00:00.0 with an elevation cut-off of 15°

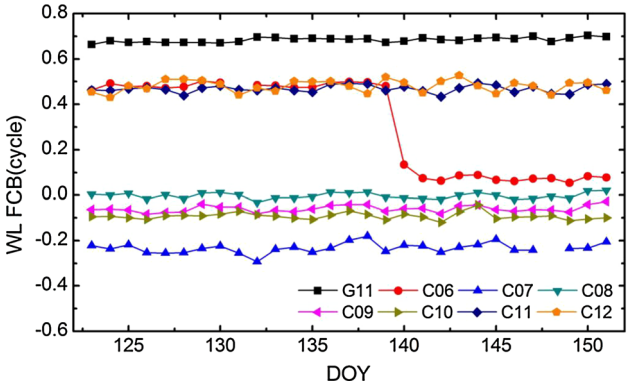

Fig. 3 Time series of daily WL FCBs from DOY 123 to 151 (May 3 to May 31), 2015. The single-differenced BDS WL FCBs are referenced to C14 and the single-differenced GPS WL FCBs are referenced to G20

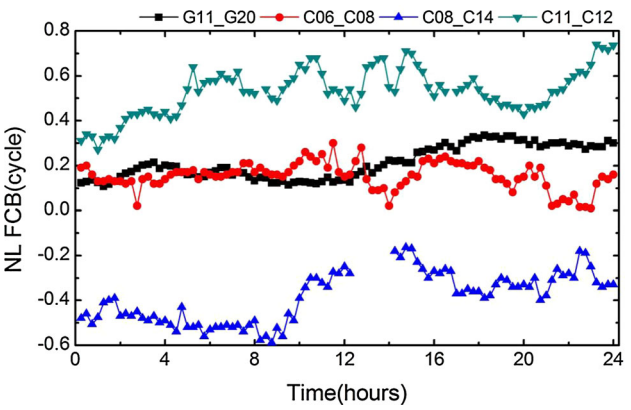

Fig. 4 Time series of four pairs of NL FCBs in each 15 min session on DOY 125, 2015

The average number of visible GPS satellites is obviously more than that of BDS satellites. However, there are still some areas where the visible number is only approximately 6–8. As expected, integrating GPS and BDS can significantly increase the visible satellite number, especially in the Asia-Pacific region. It is beneficial for the BDS NL FCB estimation because a station outside the Asia-Pacific region can often only track 2–3 BDS IGSO + MEO satellites, which cannot contribute to the BDS NL FCB estimation in single-system PPP. However, their BDS ambiguities can still be precisely estimated in dual-system PPP when integrated with GPS observations. Therefore, in dual-system PPP model, we can employ the GPS + BDS observations from the stations all over the world for GPS and BDS FCB estimation.

The temporal stability of WL/NL FCBs has an important influence on the determination of the time step-size of one session for the FCB estimation using a piece-wise-constant function. As a result of being well studied, the WL FCBs for GPS are known to be rather stable over several days, and the NL FCBs are stable within a short time span, such as 15 min (Ge et al. 2008), or for each full pass over a regional network (Geng et al. 2009). However, the temporal stability of BDS WL/NL FCBs has not been well analysed in previous studies. Figure 3 shows the time series of daily BDS WL FCBs, referenced to C14, from DOY 123 to 151, 2015. For comparison, the time series of daily GPS WL FCBs for G11, referenced to G20, are also presented in Fig. 3. These FCBs were calculated by simply averaging the fractional parts of all single-differenced ambiguities involved for each satellite pair. The overall standard deviation (STD) of WL FCBs was 0.072 cycles for GPS and 0.104 cycles for BDS. One can see that for all satellites, except C06, the daily BDS WL FCBs agreed with each other by less than 0.1 cycles. The WL FCBs of C06 suffered a datum offset on DOY 140 (May 20). We also found that the precise clock corrections of C06 provided by Wuhan University and GeoForschungsZentrum Potsdam (GFZ) experienced a datum offset on that day. The reason for the offset was not clear and needed further investigation. The change of the daily C06 WL FCBs was still less than 0.1 cycles within each sub-interval. Although the time series of the BDS WL FCBs were not as stable as those of the GPS WL FCBs, these results indicated that BDS WL FCBs can be estimated on a daily basis and can even be predicted for real-time applications with an update time interval of several days.

The NL FCBs, represented by the average of the fractional parts of all of the involved NL single-differenced ambiguities of each satellite pair in each 15-min session on DOY 125, are presented as typical examples in Fig. 4 for satellite pairs C06–C08 (IGSO pair), C08–C14 (IGSO-MEO pair), C11-C14 (MEO pair) and G11–G20. The multi-GNSS precise satellite orbits and clock products provided by GFZ were used for the calculations. The overall STD of the NL FCBs is 0.078 cycles for GPS and 0.083 cycles for BDS. As shown in Fig. 4, the change of the G11 NL FCBs was approximately less than 0.2 cycles within one day. The change did not exceed 0.05 cycles between two adjacent sessions. For BDS, the NL FCBs change can reach up to 0.3 cycles during an interval of 2 h or more. Nevertheless, the difference between two adjacent sessions was usually not over 0.1 cycles; 91.5 % of the differences were between −0.075 and 0.075 cycles. These results indicated that the BDS NL FCBs were also relatively stable over a short time span, such as 15–30 min. It is reasonable to estimate the BDS NL FCBs with a 15-min step-size.

Therefore, for both GPS and BDS, we estimated the WL FCBs on a daily basis and the NL FCBs for a 15-min time interval. Two strategies were used for quality control: (1) eliminating the input ambiguities with a high formal sigma or small number of observations and (2) rejecting the ambiguity observations with a large residual during the iterative process.

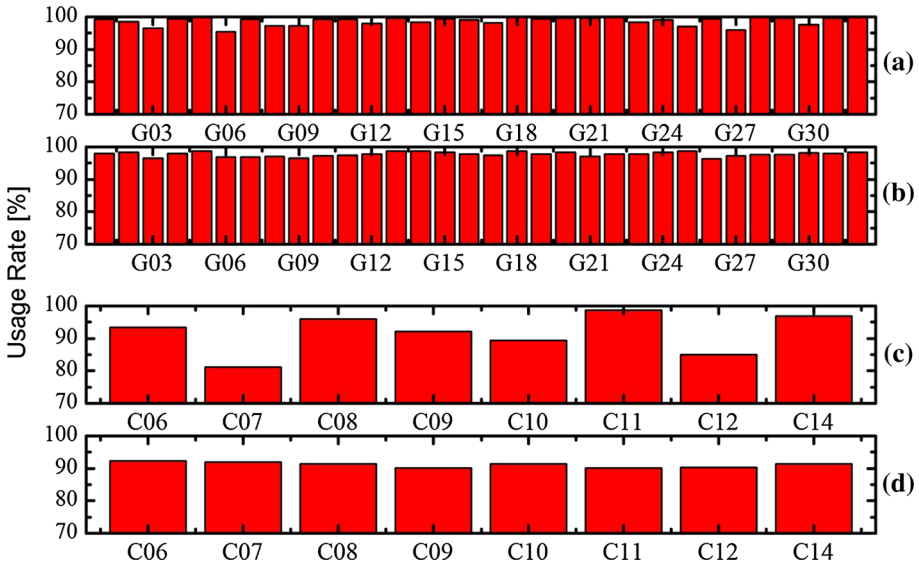

Fig. 5 Usage rate of the GPS (**a** for WL, **b** for NL) and BDS (**c** for WL, **d** for NL) float ambiguities

2.3 Quality of FCB products

The usage rate P_{ur}, i.e., the percentage of the valid float ambiguity observations used for FCB estimation, is a useful index to indicate the consistency of FCBs. It is calculated with the following formula:

$$P_{\mathrm{ur}} = \frac{N_{\mathrm{amb\_v}}}{N_{\mathrm{amb\_v}} + N_{\mathrm{amb\_r}}} \times 100.0\ \%, \tag{12}$$

where $N_{\mathrm{amb\_v}}$ is the number of input ambiguities finally contributed to FCB estimation and $N_{\mathrm{amb\_r}}$ is the number of input ambiguities rejected by the estimation due to a large residual. Figure 5 shows the average usage rate of WL and NL ambiguities for each satellite. As shown in Fig. 5, almost all of the GPS WL ambiguities are used for WL FCB estimation. The minimum and maximum usage rate reached as high as 95.4 % and 99.9 %, respectively, and the average value for all GPS satellites was 98.8 %. It was found that the usage rate of the GPS NL ambiguities is slightly lower than that of the WL ambiguities, and the minimum, maximum and average usage rates were 96.3, 98.7 and 97.8 %, respectively. For BDS, the usage rate of the WL ambiguities ranged from 81.1 to 98.7 % for an individual satellite, and the average value for all BDS satellites was 91.8 %. However, the usage rates of the C07 and C12 WL ambiguities were only 81.1 and 85.1 %, respectively, which were far lower than the average value. This may be related to the inaccurate BDS code bias variation correction model, which would be reflected in the residuals of the C07 and C12 satellites. The correction model proposed by Wanninger and Beer (2015) could be further improved by estimating independent parameters for each of the IGSO + MEO satellites with more observations or by providing the precision information for the corrections. The minimum, maximum and average usage rate of the BDS NL ambiguities were 90.1, 92.2 and 91.1 %, respectively. All of the BDS satellites showed almost the same usage rate of NL ambiguities, indicating a similar quality level of NL ambiguities amongst the BDS satellites, which was different from the WL ambiguities. This was reasonable because the NL float ambiguities were mainly derived from carrier-phase measurements over a long period with a much larger weight compared to code observations, and thus, they were not seriously affected by BDS code biases. By comparing the usage rates between GPS and BDS, it was found that the GPS WL and NL ambiguities had a better consistency and precision than the BDS ambiguities.

The posteriori residual of Eq. (11) (that is, $R_{\mathrm{r}}^{\mathrm{s}} - (\hat{d}_{\mathrm{r}} - \hat{d}^{\mathrm{s}})$, where $\hat{d}_{\mathrm{r}}$ and $\hat{d}^{\mathrm{s}}$ are the FCB estimates at receiver and satellite end, respectively) also provides an internal precision indicator for FCB estimates. Figure 6 shows the residual distributions of all of the GPS and BDS FCB solutions. The RMS of the GPS WL residual was 0.074 cycles, while that of the GPS NL residuals was 0.079 cycles. This was attributable to the fact that GPS NL FCB estimates were more sensitive to unmodelled errors due to its shorter wavelength. On the contrary, the BDS NL residuals showed a smaller RMS value than the BDS WL residuals. The large RMS of the BDS WL ambiguities can be attributed to the code bias variations, as discussed previously. Again, by comparing the residuals between GPS and BDS, it is shown that the precision of BDS FCB is worse than that of GPS.

From the results of the usage rates as well as the residual distributions, we conclude that the overall performance of FCB can be expressed by the following inequality:

$$\mathrm{WL(G)} > \mathrm{NL(G)} > \mathrm{NL(C)} > \mathrm{WL(C)}$$

We also performed the BDS WL FCB estimation without code bias corrections. The average usage rate for all of the

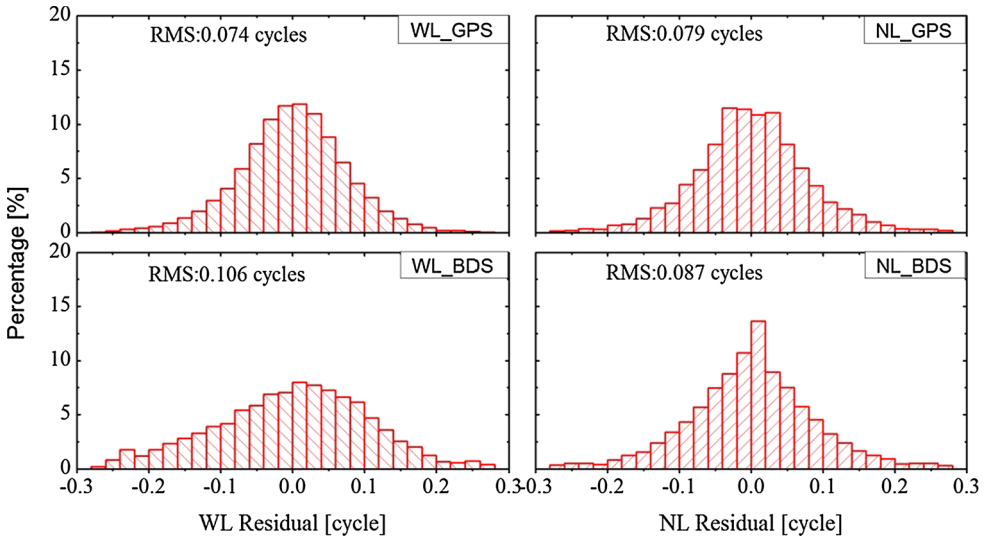

Fig. 6 Residual distributions of the WL and NL ambiguity bias (cycle) for GPS (*upper panel*) and BDS (*bottom panel*)

BDS satellites dramatically decreased to 80.4 %, and the RMS of BDS WL residual increased to 0.113 cycles, thus further demonstrating that the code bias variations have an important influence on BDS WL FCB estimation and must be corrected to produce high-quality BDS WL FCB estimates.

3 PPP AR processing strategy

At user end, the single-differenced ambiguities between satellites are formed and aimed to be fixed in our PPP procedure. The satellite with the highest elevation angle and continuous observations of more than 5 min would be selected as the reference satellite to form the single-differenced ambiguities. The inter-system ambiguity between GPS and BDS cannot be fixed to an integer because of the different wavelengths of the GPS and BDS signals. Therefore, one GPS and one BDS IGSO (or MEO) satellite were chosen as the references to form inner-system ambiguities for the GPS + BDS dual-system AR.

Generally, PPP AR at the user end was conducted in two sequential steps. First, the WL ambiguities from MW combination were corrected with WL FCBs and aimed to be fixed. If WL ambiguities were successfully fixed, then the NL ambiguities were derived according to Eq. (8) and aimed to be fixed with NL FCBs corrected. As is well discussed in the literatures (Geng et al. 2010; Collins et al. 2008; Laurichesse et al. 2009), the single-differenced smoothed WL ambiguities can be easily fixed by rounding each epoch. For the single-differenced NL AR, a search strategy based on the Least-squares AMBiguity Decorrelation Adjustment (LAMBDA) method (Teunissen 1995) was applied to search for the optimal integer solution.

The ambiguities need to be fixed correctly. In theory, it is better to have as many correctly fixed ambiguities as possible. However, in some cases, some GNSS models may not be strong enough to resolve the full vector of integer ambiguities with a sufficiently high success rate. With the PPP PAR method proposed by Li and Zhang (2015), Teunissen et al. (1999) and Wang and Feng (2013), we can split the decorrelated ambiguity vector into a part that is not fixed and a part that is fixed:

$$\underbrace{\begin{bmatrix} \hat{z}_p \\ \hat{z}_{n-p} \end{bmatrix}}_{\hat{z}} = \underbrace{\begin{bmatrix} Z_p \\ Z_{n-p} \end{bmatrix}}_{Z} \hat{a} \tag{13}$$

with

$$\hat{a} = \left[\hat{a}(\mathrm{G}),\ \hat{a}(\mathrm{C})\right], \tag{14}$$

where $\hat{a}$ is the real-valued solution of the ambiguity vector, which consists of the GPS component $\hat{a}(\mathrm{G})$ and the BDS component $\hat{a}(\mathrm{C})$; $\hat{z}_p$ being the decorrelated subset that is fixed to integers and $\hat{z}_{n-p}$ being the subset that is kept as real-valued parameters, they are transformed from $\hat{a}$ by the integer matrix Z_p and Z_{n-p}, respectively. The partially fixed integer solution can be obtained through the integer least-squares search of the LAMBDA method.

For a successful IF AR, the WL FCBs are used only for resolving the WL ambiguities while the NL FCBs would be introduced in the carrier phase observation equation of PPP. This is because that the integer-recovered IF ambiguity consists of the integer WL and NL single-differenced ambiguity, and the NL FCB. The NL FCB estimates, besides integer single-differenced ambiguity estimates, directly contribute to the ambiguity-fixed PPP solutions. Therefore, the accuracy

Table 1 Site information of six user stations

Site name	Rec type	Ant type	AVS (GPS)	AVS (BDS IGSO + MEO)
CUT0	TRIMBLE NETR9	TRM59800.00 SCIS	8.7	4.6
JFNG	TRIMBLE NETR9	TRM59800.00 NONE	8.7	4.6
NRMG	TRIMBLE NETR9	TRM57971.00 TZGD	8.9	3.5
SPA7	JAVAD TRE_G3T DELTA	TRM59800.00 SCIS	8.6	4.4
WARK	TRIMBLE NETR9	TRM55971.00 NONE	8.4	3.3
XMIS	TRIMBLE NETR9	TRM59800.00 NONE	9.3	5.8

The information includes the name, receiver type, antenna type, average visible satellite number per epoch (AVS) of GPS and BDS IGSO + MEO

of the NL FCB has a significant effect on the PPP ambiguity-fixed solution (Geng et al. 2011). Hence, a practical way of using the single-differenced integer solution information is to apply a tight constraint on the ambiguity parameters. The constraint is applied as a pseudo-observation in the estimation, which treats the single-differenced integer ambiguities as observations of the ambiguity parameters in the filter. One can weight the pseudo-observation according to the accuracy of the NL FCB. This strategy has been used by Geng et al. (2011) for ambiguity-fixed PPP and by Takasu and Yasuda (2010) for double-differenced AR. In this study, the standard deviations of GPS and BDS NL FCB are set to 0.05 cycles and 0.08 cycles, respectively.

The GPS + BDS observations, recorded at 30 s sampling intervals from IGS MGEX, were used to validate the effectiveness of the GPS + BDS PPP AR. Figure 1 shows the distribution of the GPS + BDS reference network and user stations. Approximately 70 stations were used for FCB estimation. Six stations denoted by red stars were used for the PPP tests. Site information for six user stations, including the site name, receiver type, antenna type and average visible satellite number per epoch (AVS), were summarized in Table 1. The daily observations from DOY 123 to 151, 2015, were used in this study. The combined precise GPS and BDS satellite orbit and clock products provided by GFZ (Deng et al. 2014) were used, and the corresponding FCB products were estimated and employed for the PPP tests. Due to a relatively large day boundary bias, caused by orbit discontinuity in the precise satellite orbit, the calculated precise orbit suffered from a large interpolation error at the start and end time periods (Griffiths and Ray 2009; Lou et al. 2014). Therefore, for each station, only the GPS and BDS observations during the period of GPS time 02:00–22:00 were used for data processing.

We applied the absolute antenna phase centres model and the phase wind-up corrections (Wu et al. 1993). To maintain consistency with the GBM precise products, the satellite PCO + PCV corrections estimated by ESA were applied for BDS while "igs08.atx" were used for GPS PCO + PCV corrections (Schmid et al. 2007). Because the receiver PCO and PCV corrections for BDS signals were not available at this time, we simply used GPS corrections for BDS signals, which is consistent with the strategy for BDS precise orbit determination and clock estimation (Li et al. 2015b; Lou et al. 2014). In addition, the elevation-dependent BDS satellite-induced code biases were corrected according to Wanninger and Beer (2015). The elevation cut-off angle was set to 10°. The elevation-dependent weighting scheme of observations applied in this research to mitigate the effects of multipath as well as atmospheric errors is given as

$$\sigma^2 = a^2 + a^2/\sin^2(\mathrm{el}),$$

where σ is the standard deviation of the GPS and BDS measurements and el is the elevation angle of the satellite. The values of a for the GPS and BDS carrier phase observations were set to 3 mm. The values of a for the GPS, BDS IGSO + MEO and BDS GEO code observations were set to 0.3, 0.6 and 3.0 m, respectively. We validated the integer ambiguity solutions using two popular indexes: the bootstrapping success rate and the ratio-test (Ji et al. 2010). The critical criteria of the success rate and ratio value were selected as 0.99 and 2.0, respectively. Only when the requirement of the success rate and the ratio test has been satisfied, the integer ambiguities would be accepted.

4 PPP AR results

The PPP AR performance in terms of TTFF and the fixing rate of three groups of solutions (BDS-only, GPS-only and GPS + BDS PPP AR) would be compared and analysed. The TTFF was defined as the time taken for the ambiguity-fixed solution to be successfully achieved (Feng and Wang 2008; Gao et al. 2015). We analysed the fixing rate based on the results after the first fixing solution was achieved. The fixing rate was defined as the ratio of the number of fixed epochs to the number of total epochs during this period, as in Li and Zhang (2015).

Additionally, we would compare the convergence time (CT) and position performance of three groups of solutions. In this study, convergence is defined as the time required to

attain a 3D positioning error less than 10 cm, which had been adopted by Jokinen et al. (2011) and Li and Zhang (2014). The positioning error was the difference between the position solution and the reference coordinate from the GPS network solution with BERNESE 5.0 software (Dach et al. 2007). The solution was required to have a position error of less than 10 cm for 20 epochs for convergence to be attained. The position performance, represented by average, standard deviation (STD), root mean square (RMS), maximum (MAX) values of the positioning errors, in easting (E), northing (N) and up (U) component, would be assessed for both static and kinematic ambiguity-fixed PPP solutions. For static PPP, the position performance for 1 h observations (GPS time 02:00-03:00) was analysed whether the convergence was achieved or not, because in many emerging applications only a relatively short observation period, such as one hour, can be provided (Geng et al. 2009). For kinematic PPP, the static data from user stations were processed in simulated kinematic mode and the position performance after convergence was analysed.

4.1 Static tests

The TTFF of each static PPP solution is recorded, and the statistical results for all cases are given in Table 2. We found that the TTFF for the NRMG and WARK stations were much longer for the other stations, particularly in the case of BDS PPP AR. This is because the average number of observed BDS satellites for these two stations is less than that of the other four stations, as shown in Table 1. On the contrary, XMIS achieves the fastest TTFF of BDS ambiguity fixing because it has the most tracked BDS IGSO + MEO satellites among the six stations. However, the BDS TTFF for XMIS is almost as long as 3h. Generally, the TTFF of BDS PPP-AR requires up to several hours. Compared with the results of BDS ambiguity fixing, the TTFF of GPS ambiguity fixing is much shorter. Approximately 20 min is required to achieve the first GPS fixed solution. The GPS TTFFs of six stations are close to each other because that these stations can observe almost the same number of GPS satellites. Among the three groups of solutions, the combined PPP AR with GPS + BDS achieves the fastest TTFF of approximately 15–20 min. Compared to the results of GPS ambiguity fixing, the average TTFF can be further shortened by approximately 22.1 % in GPS + BDS PPP AR.

Table 3 summarizes the statistics of the fixing rate for three groups of static PPP solutions. As shown in Table 3, the fixing rate of BDS-only PPP AR is less than 35 % for all test stations except for XMIS. This is reasonable once we acknowledge the fact that the number of BDS IGSO and MEO tracked satellites is quite limited for most areas. At present, even in the Asia-pacific region, the number of BDS IGSO + MEO satellites is often no more than 6. The average number of visible BDS IGSO + MEO satellites for NRMG and WARK is less than 4, resulting in a much smaller BDS fixing rate. Among all six stations, XMIS achieves the best performance, with a fixing rate of 60.3 % for BDS-only PPP AR. The fixing rate of GPS-only PPP AR ranges from 97.5 to 99.6 % for these test stations. Compared with GPS-only PPP AR, the fixing rate can be further increased by dual-system PPP AR. It is observed that the GPS + BDS ambiguity fixing rate is always higher than that of GPS-only case for all test stations. The highest average fixing rate of 99.5 % is achieved by the GPS + BDS combined PPP AR.

Figure 7 shows a typical convergence for BDS, GPS, GPS + BDS PPP in static mode, taking the results for station CUT0, on DOY 123, 2015, as example. The CT is 117.5, 20.5 and 18 min for BDS, GPS, GPS + BDS static PPP, respectively. The statistics of average, MIN and MAX CT of static PPP for each station are given in Table 4. For BDS-only PPP, it usually takes over 100 min to obtain a 3D position error less than 1 dm. However, the MIN values of BDS CT are often less than 30 min. This indicates that it is still possible to achieve a relatively fast convergence when the number of observed BDS satellites is many enough, for example, the number of BDS IGSO + MEO satellite is over 6. The CT of GPS PPP AR is often 20–40 min, which is much faster than that of BDS-only solutions. The fastest convergence can be achieved in GPS + BDS PPP AR. The statistical results of CT for three groups of solutions are as follows: in static PPP with AR, the average CT is 172.6 min for BDS, 22.3 min for GPS while only 17.9 min for GPS + BDS. Compared with

Table 2 The average TTFF (min) for static PPP AR

	BDS	GPS	GPS + BDS
CUT0	523.3	22.4	16.0
JFNG	189.8	17.5	13.4
NRMG	703.6	26.5	18.8
SPA7	563.9	18.7	16.2
WARK	1013.6	27.4	21.3
XMIS	162.1	17.6	15.6
AVE	526.1	21.7	16.9

Table 3 The average fixing rate (%) for static PPP AR

	BDS	GPS	GPS + BDS
CUT0	33.7	99.4	99.8
JFNG	25.9	98.8	99.5
NRMG	11.6	98.5	99.1
SPA7	27.3	99.6	99.8
WARK	13.5	97.5	99.3
XMIS	60.3	97.9	99.7
AVE	28.7	98.6	99.5

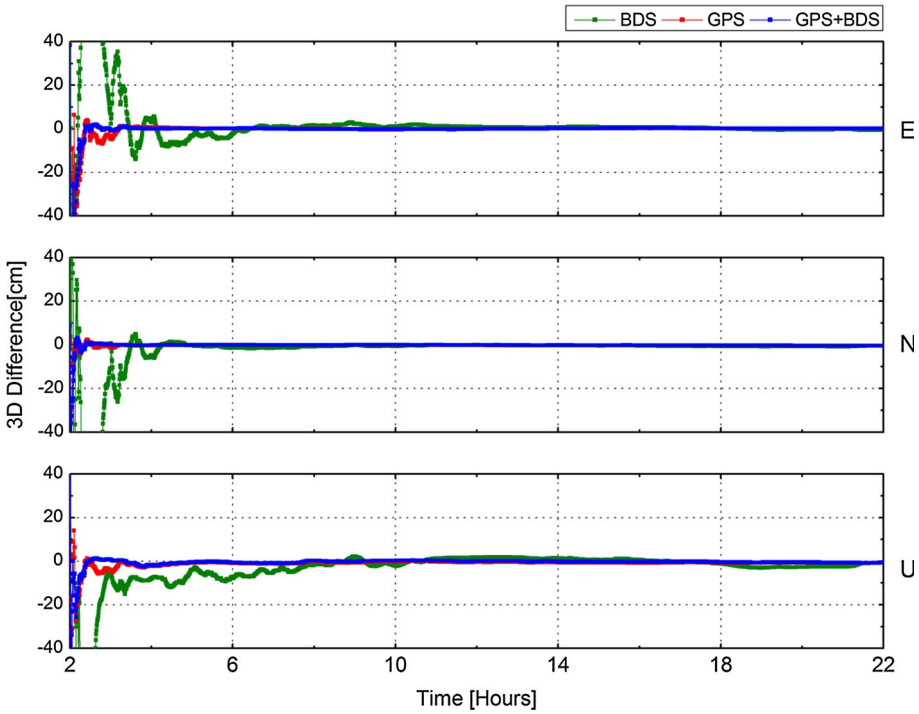

Fig. 7 Position differences for BDS, GPS, GPS + BDS PPP in static mode, at station CUT0, on DOY 123, 2015

Table 4 Overview of convergence time for static PPP AR

	Average			Min			Max		
	BDS	GPS	GPS + BDS	BDS	GPS	GPS + BDS	BDS	GPS	GPS + BDS
CUT0	102.1	18.1	14.9	20.0	5.0	6.0	304.5	34.0	26.0
JFNG	73.9	15.1	13.2	11.0	7.0	7.0	124.0	39.5	30.0
NRMG	340.8	27.8	23.0	13.5	10.5	9.0	771.0	70.0	59.0
SPA7	101.7	13.5	13.1	19.5	6.0	5.0	226.5	32.0	29.0
WARK	307.6	30.7	23.2	34.5	10.0	10.0	781.5	60.5	50.0
XMIS	109.3	28.5	20.2	25.5	13.0	9.5	373.5	81.0	62.0

Convergence time is presented in units of minutes

Table 5 The average position error of static PPP AR for 1 h observations

	BDS			GPS			GPS + BDS		
	E	N	U	E	N	U	E	N	U
CUT0	−6.4	−0.3	−13.8	−0.5	0.3	−1.3	−0.5	0.4	−0.9
JFNG	−0.7	1.4	−2.6	0.2	0.4	0.4	0.2	0.6	0.0
NRMG	15.6	5.8	−35.7	−0.4	0.0	3.2	−0.5	0.0	2.2
SPA7	−6.0	1.5	−8.8	−0.7	0.1	−0.8	−0.3	0.1	−0.6
WARK	28.1	0.3	−18.0	−2.5	0.4	3.1	−0.8	−0.1	2.4
XMIS	1.6	−1.4	−2.8	−0.4	−1.3	−2.7	0.3	−0.9	−2.2

All units are in cm

result of GPS, the average CT is further reduced by 19.5 % in dual-system PPP AR.

The positioning accuracy information of 1 h static PPP AR for each station over all test days is given in Tables 5, 6, 7 and 8. One can see that currently BDS static PPP can only achieve a position accuracy of tens of centimetres in horizontal and close to 1m in vertical component, respectively. It should be noted that for most instances, only ambiguity-float solution can be obtained for BDS hourly PPP, because that the TTFF of BDS-only ambiguity fixing is often longer than 3 h. For GPS PPP AR, generally, the hourly position error is several centimetres in E, N and U components. The STDs

Table 6 The position error STD of static PPP AR for 1 h observations

	BDS			GPS			GPS + BDS		
	E	N	U	E	N	U	E	N	U
CUT0	24.2	5.3	26.1	1.4	0.5	2.1	1.1	0.5	1.6
JFNG	8.1	5.5	11.1	1.2	1.0	2.9	0.9	1.1	2.3
NRMG	26.7	8.7	46.6	4.6	0.9	5.4	1.5	0.8	3.6
SPA7	13.0	4.8	11.8	1.2	0.5	2.0	1.0	0.6	1.8
WARK	39.5	15.1	61.7	5.6	2.0	5.8	1.9	1.1	2.7
XMIS	21.2	9.9	16.7	4.1	1.3	3.6	1.9	1.3	2.7

All units are in cm

Table 7 The position error RMS of static PPP AR for 1 h observations

	BDS			GPS			GPS + BDS		
	E	N	U	E	N	U	E	N	U
CUT0	25.0	5.3	29.5	1.4	0.6	2.5	1.3	0.6	1.9
JFNG	8.2	5.7	11.4	1.3	1.1	2.9	0.9	1.2	2.3
NRMG	30.9	10.5	58.7	4.7	1.0	6.2	1.6	0.8	4.2
SPA7	14.4	5.0	14.7	1.4	0.5	2.1	1.1	0.6	1.9
WARK	48.5	15.1	73.4	6.5	2.1	7.0	2.1	0.9	3.6
XMIS	21.3	10.0	17.0	4.2	1.8	4.9	2.0	1.5	4.2

All units are in cm

and RMSs of NRMG, WARK and XMIS are much larger than other stations because there are some days the GPS ambiguities cannot be successfully fixed with hourly data for these stations. The position accuracy of ambiguity-float PPP is often lower than that of ambiguity-fixed PPP (Geng et al. 2009; Li et al. 2015a). For dual-system PPP, there are more observations used for estimation and the probability of successful AR within 1 h is much higher than the single-system PPP. Therefore, the hourly position accuracy can be much improved. Compared with the results of GPS PPP, the average RMSs of all stations are improved from (3.3, 1.2, 4.3) cm to (1.5, 0.9, 3.0) cm in GPS + BDS PPP, with an improvement of 54.5, 25.0 and 30.2 % in E, N and U component, respectively.

Table 9 The average TTFF (min) for kinematic PPP AR

	BDS	GPS	GPS + BDS
CUT0	564.6	33.2	24.0
JFNG	346.9	24.6	16.4
NRMG	848.6	43.9	25.3
SPA7	627.6	32.1	25.4
WARK	1107.8	44.6	39.6
XMIS	211.2	23.1	17.2
AVE	617.8	33.6	24.6

4.2 Kinematic tests

For kinematic PPP, a random walk process is used to model the dynamics of the vehicle in the kalman filter. The same spectral density values are used as in the static case, except that a value of 10^4 m^2/s is used for the position coordinates. Table 9 presents the statistical TTFF of the kinematic PPP AR tests. The performance of the BDS-only PPP AR shows the longest TTFF, whereas GPS + BDS PPP AR shows the shortest TTFF. In general, the TTFF of BDS PPP-AR is over 9 h. Such a long TTFF extremely limits the application of BDS kinematic PPP AR. In the case of GPS-only PPP AR, approximately 25–45 min is required to achieve the first fixed solution, a much shorter TTFF than that for BDS. The dual-system PPP AR achieves the fastest TTFF among all three groups of solutions, approximately 20–40 min. Compared with the results of GPS-only PPP AR, the average TTFF can be shorten by about 26.8 % with GPS + BDS PPP AR. Moreover, it is observed that the average GPS TTFF has a better consistency among the six stations than the BDS TTFF. This is attributed to the fact that the number of visible GPS satellite is sufficient and roughly close to each other among all of the selected stations because of the homogeneous global coverage of GPS. However, the situations are different for BDS-based PPP for an individual station. By comparing the results given in Tables 2 and 4, we note that the TTFF for kinematic PPP is obviously longer than that for static PPP.

Table 8 The MAX position error of static PPP AR for 1 h observations

	BDS			GPS			GPS + BDS		
	E	N	U	E	N	U	E	N	U
CUT0	−54.7	21.1	−82.9	3.9	−1.6	−5.9	−2.4	1.7	−5.5
JFNG	−35.2	24.4	−23.2	2.6	−3.5	7.6	1.8	3.2	−6.0
NRMG	47.5	−19.8	60.3	8.5	2.8	12.1	3.1	−1.7	12.3
SPA7	−28.4	15.4	−41.5	−3.2	8.7	5.1	−2.1	1.3	4.6
WARK	70.1	−43.3	−88.7	−19.5	8.2	−27.3	−11.4	5.7	−8.4
XMIS	54.3	−27.6	61.2	−10.2	−5.8	−10.8	8.2	−3.4	−11.3

All units are in cm

Table 10 The average fixing rate (%) for kinematic PPP AR

	BDS	GPS	GPS + BDS
CUT0	29.3	97.9	99.5
JFNG	23.7	97.7	99.2
NRMG	11.5	93.6	97.1
SPA7	20.6	98.4	99.7
WARK	10.1	96.8	99.1
XMIS	61.3	97.8	99.3
AVE	26.1	97.0	99.0

The statistical results of the fixing rate for three groups of kinematic PPP solutions are summarized in Table 10. Solutions of BDS-only PPP with ambiguity fixing have a very low fixing rate, often less than 30.0 % except for station XMIS. These results show that the BDS ambiguity can only be fixed for a few epochs in kinematic PPP with the current BDS constellation. The fixing rate of GPS-only ambiguity-fixed PPP solution is generally over 93 %. The fixing rate of dual-system PPP AR can be further increased to approximately 99.0 %, which guarantees the accuracy and reliability of kinematic PPP. One can find that for all test stations, the fixing rate of dual-system PPP AR is always higher than that of single-system PPP AR. Moreover, comparing the results given in Tables 3 and 10, we can also see that the fixing rate in kinematic PPP is obviously lower than that in static PPP due to the weaker strength of the kinematic PPP model.

Figure 8 shows a typical convergence for BDS, GPS, GPS + BDS PPP in kinematic mode, taking the results for station JFNG, on DOY 151, 2015, as example. The CT is 105, 32.5 and 22.5 min for BDS, GPS, GPS + BDS kinematic PPP, respectively. The statistics of average, MIN and MAX CT of kinematic PPP for each station are given in Table 11. By comparing Tables 4 and 11, one can see that, owing to a relatively weaker model (indicated by much more parameters estimated in kinematic PPP), the average CT of kinematic

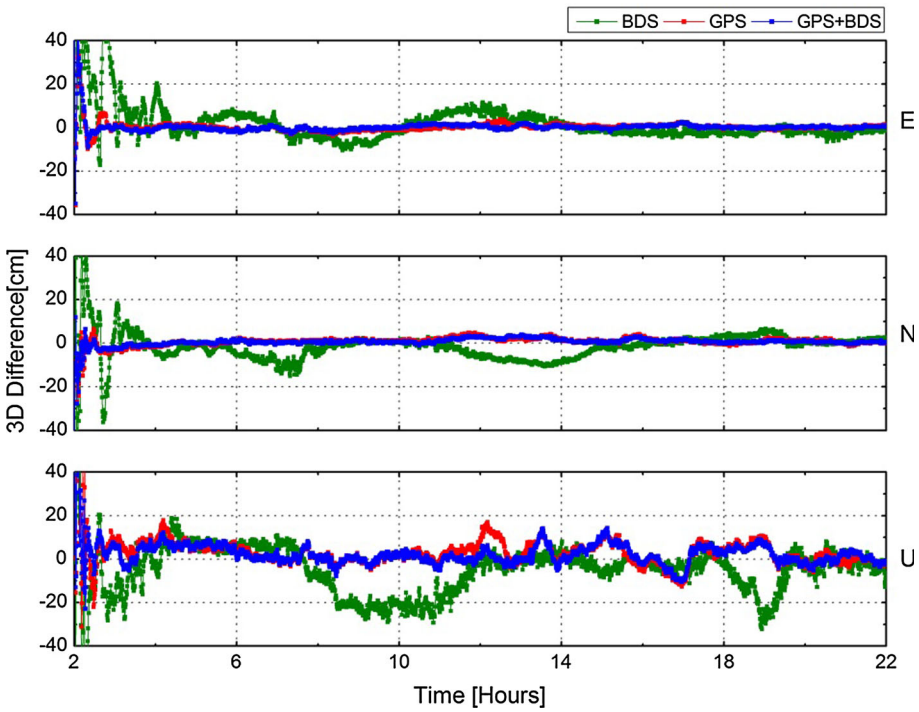

Fig. 8 Position differences for BDS, GPS, GPS + BDS PPP in kinematic mode, at station JFNG, on DOY 151, 2015

Table 11 Overview of convergence time for kinematic PPP AR

	AVERAGE			MIN			MAX		
	BDS	GPS	GPS + BDS	BDS	GPS	GPS + BDS	BDS	GPS	GPS + BDS
CUT0	159.3	35.5	22.4	20.5	11.5	11.5	529.0	70.5	55.5
JFNG	82.5	24.9	19.6	18.0	11.5	7.0	181.5	57.0	54.5
NRMG	517.0	41.8	29.8	25.0	23.0	13.5	912.0	75.5	60.0
SPA7	158.2	22.7	16.6	26.5	10.0	7.0	472.0	51.0	30.0
WARK	657.8	45.5	28.7	69.0	18.5	13.5	922.0	82.0	60.0
XMIS	152.6	32.3	22.1	20.0	12.5	9.5	848.5	86.5	75.0

Convergence time is presented in units of minutes

Table 12 The average position error of kinematic PPP AR

	BDS			GPS			GPS + BDS		
	E	N	U	E	N	U	E	N	U
CUT0	2.8	0.4	−3.5	0.2	−0.2	0.6	0.4	−0.1	0.0
JFNG	−0.7	0.7	−9.6	0.2	0.4	1.0	−0.3	0.5	−0.1
NRMG	2.4	2.4	−0.4	−0.7	−0.4	0.3	1.1	0.6	0.0
SPA7	2.4	0.3	−2.0	0.2	−0.3	0.7	0.3	−0.2	0.4
WARK	2.1	−0.9	0.1	0.3	−0.1	0.1	0.3	−0.2	0.5
XMIS	0.6	−1.1	−6.1	−0.5	−0.8	−2.6	−0.3	−0.8	−1.8

All units are in cm

Table 13 The position error STD of kinematic PPP AR

	BDS			GPS			GPS + BDS		
	E	N	U	E	N	U	E	N	U
CUT0	3.6	3.4	11.7	1.0	0.8	3.9	0.9	0.7	3.5
JFNG	4.5	3.5	10.6	1.4	1.2	4.0	0.9	0.9	3.2
NRMG	8.8	9.5	15.4	3.0	2.0	7.2	2.9	2.5	6.7
SPA7	4.1	4.0	10.8	0.9	0.8	3.4	0.9	0.8	3.3
WARK	9.5	7.5	14.8	1.0	1.0	4.3	1.0	0.9	3.9
XMIS	3.0	1.9	10.9	1.9	1.4	5.8	1.1	0.9	4.5

All units are in cm

Table 14 The position error RMS of kinematic PPP AR

	BDS			GPS			GPS + BDS		
	E	N	U	E	N	U	E	N	U
CUT0	4.8	3.8	12.5	1.1	0.8	4.0	1.0	0.7	3.6
JFNG	4.7	3.8	14.7	1.5	1.3	4.3	1.0	1.0	3.3
NRMG	10.8	10.6	16.9	4.4	2.6	7.5	3.9	2.9	7.0
SPA7	5.0	4.4	11.5	1.0	0.9	3.5	1.0	0.8	3.5
WARK	11.0	8.3	15.7	1.1	1.0	4.3	1.1	1.0	4.0
XMIS	3.3	2.2	12.7	2.1	1.7	7.3	1.2	1.3	6.6

All units are in cm

PPP is significantly longer than that of static PPP. For BDS-only PPP, it usually takes over 150 min to obtain a 3D position error less than 1 dm. For NRMG and WARK, the CT can be longer than 15 h in the worst cases. The CT of GPS PPP AR is often 30–50 min, which is much faster than that of BDS PPP. For each station, the convergence speed of GPS + BDS PPP AR is always the fastest. The statistical results of CT for three groups of solutions are as follows: in kinematic PPP with AR, the average CT is 287.9 min for BDS, 33.8 min for GPS while only 23.2 min for GPS + BDS. Compared with result of GPS, the average CT is further reduced by 31.3 % in dual-system PPP AR.

The kinematic PPP positioning accuracy information, represented by average, STD, RMS and MAX values of epoch-wise positioning errors after convergence for each station over all test days, is shown in Tables 12, 13, 14 and 15, respectively. From the average, STD and RMS results, one can see that the accuracy of BDS kinematic PPP is about 1 dm in E, N and 1–2 dm in U component. For GPS PPP AR, the absolute values of position errors are generally less than 1 dm in E, N and 2 dm in U component, respectively. The GPS PPP AR has average RMS values of 1.9, 1.4 and 5.2 cm in E, N and U directions, which means that the GPS kinematic PPP AR can achieve an accuracy of 1–2 cm in horizontal and about 5 cm in vertical components at the one-sigma level. Dual-system PPP AR can further improve the kinematic positioning accuracy and has average RMSs of 1.5, 1.3 and 4.7 cm. Compared with the results of GPS PPP AR, the average RMSs of all stations are further reduced by 21.1, 7.1 and 9.6 %, respectively.

5 Conclusions and remarks

This study realizes an effective GPS + BDS FCB estimation based on GPS + BDS combined PPP with observations from MGEX. The treatment and performance of BDS FCB estimation are provided in details. The combined FCB estimation outperforms single-system estimation because (1) more stations can contribute to the estimation and (2) the FCB precision is probably higher with the more accurate float ambiguities estimated in combined PPP. It should be noted that the FCBs of BDS GEO satellites are not estimated

Table 15 The MAX position error of kinematic PPP AR

	BDS			GPS			GPS + BDS		
	E	N	U	E	N	U	E	N	U
CUT0	−21.8	−27.9	43.2	9.3	−6.3	20.2	6.1	−6.0	−22.1
JFNG	18.2	24.6	−25.0	10.9	−10.3	17.7	−9.8	10.9	17.7
NRMG	−35.0	−33.5	39.5	11.3	−9.8	24.3	10.5	−10.1	−19.3
SPA7	27.8	−19.1	−38.7	−10.9	12.9	−22.3	−9.6	11.5	−21.6
WARK	19.9	−28.1	41.0	6.2	−8.9	−18.7	8.9	−9.2	17.5
XMIS	−21.0	−18.0	38.4	−17.7	10.3	21.1	8.4	−9.3	−18.7

All units are in cm

herein considering the low-precision orbit products for BDS GEO. In addition, it is difficult to correct the satellite-induced pseudorange variations for BDS GEO satellites.

Based on the GPS + BDS FCB estimates, we realize the GPS + BDS combined PPP AR. For dual-system AR, one GPS and one BDS IGSO or MEO satellite with the highest elevation angle and continuous observations of more than 5 min are chosen as reference satellites to form inner-system single-differenced ambiguities. The single-differenced GPS and BDS NL ambiguities can then be fused by the PAR strategy to increase the possibility of fixing a subset of decorrelated ambiguities with high confidence when FAR fails. The GPS + BDS PPP AR estimation is superior to the single-system estimation because (1) the precision of GPS or BDS ambiguity parameters would be improved in dual-system PPP so that they are more likely to be successfully fixed and (2) the probability of fixing a sufficient number of ambiguities or their linear combination can be further increased because more ambiguities are intended to be fixed in combined PPP.

GPS + BDS data collected from approximately 75 IGS MGEX stations during the period of DOY 123 to 151, 2015, are used to analyse the performance of GPS + BDS PPP AR in terms of the time to first fix and fixing rate. The performance of PPP AR was evaluated at 6 stations while the remaining stations were used to compute FCBs. Numerous experimental results show that BDS FCB estimation and BDS-only PPP AR can now be achieved. However, the quality of the BDS FCB estimates and the performance of BDS PPP AR are far worse than those of GPS. The quality and performance are limited by several factors, including the lack of precise BDS PCO+PCV corrections for receivers, the poor precision of BDS precise satellite orbits compared with GPS orbits, the smaller number of BDS IGSO + MEO satellites compared with GPS and the unbalanced coverage of the BDS constellation. BDS FCB estimates and PPP AR are expected to be refined when a more precise error correction model for BDS is proposed and when more BDS satellites come into service.

For BDS PPP-AR, several hours are required to achieve the first fixed solution, and the fixing rate is usually less than 35 % in both static and kinematic PPP tests. For GPS PPP-AR, the TTFF is approximately 20 min and 30 min, with fixing rates of 98.6 and 97.0 %, in static and kinematic PPP, respectively. In general, GPS + BDS combined PPP with ambiguity fixing shows the best performance in terms of both TTFF and the fixing rate. The average TTFF reaches 16.9 min and 24.6 min, with fixing rates of 99.5 and 99.0 %, in static and kinematic GPS + BDS PPP, respectively. Results also show that GPS + BDS PPP AR outperforms single-system PPP AR in terms of convergence time and position accuracy.

Although this study was concerned with GPS and BDS dual-frequency observations, the GLONASS, GALILEO and QZSS observations can also be integrated with the proposed method to achieve a better PPP AR performance. It is expected that with benefits from the further development of BDS in the near future, together with the further promotion of IGS MGEX, not only dual- but also multi- system PPP AR can perform better for scientific and practical applications. Moreover, the use of an additional (third) frequency is expected to improve the obtained results.

Acknowledgements This study was supported by the National Natural Science Foundation of China (Grant Nos. 41474025, 41374035, 41304005), Natural Science Foundation for Distinguished Young Scholar of Hubei Province (No: 2015CFA039), Changjiang Scholars program. The authors are grateful to the many individuals and organizations worldwide who contribute to the International GNSS Service. Special thanks to Tomoji Takasu, who developed the open source RTKLIB software for reference.

References

Boehm J, Niell A, Tregoning P, Schuh H (2006) Global mapping functions (GMF): a new empirical mapping function based on numerical weather model data. Geophys Res Lett 33:L07304. doi:10.1029/2005GL025546

Chen JP, Zhang YZ, Wang JG, Yang SN, Dong DN, Wang JX, Qu WJ, Wu B (2015) A simplified and unified model of multi-GNSS precise point positioning. Adv Sp Res 55(1):125–134

Collins P, Lahaye F, Héroux P, Bisnath S (2008) Precise point positioning with ambiguity resolution using the decoupled clock model. In: Proceedings of ION GNSS 2008. Institute of Navigation, Savannah, Georgia, pp 1315–1322

Dach R, Hugentobler U, Fridez P, Meindl M (2007) Bernese GPS Software Version 5.0. Astronomical Institute, University of Bern, Switzerland

Deng Z, Zhao Q, Springer T, Prange L, Uhlemann M (2014) Orbit and clock determination-BeiDou. In: IGS workshop, Pasadena, USA, 23–27 June 2014

Feng Y, Wang J (2008) GPS RTK performance characteristics and analysis. J Glob Position Syst 7(1):1–8

Gao W, Gao C, Pan S, Wang D, Deng J (2015) Improving ambiguity resolution for medium baselines using combined GPS and BDS dual/triple-frequency observations. Sensors 15(11):27525–27542

Ge M, Gendt G, Rothacher M, Shi C, Liu J (2008) Resolution of GPS carrier-phase ambiguities in precise point positioning (PPP) with daily observations. J Geod 82(7):389–399

Geng J, Bock Y (2013) Triple-frequency GPS precise point positioning with rapid ambiguity resolution. J Geod 87(5):449–460

Geng J, Teferle FN, Shi C, Meng X, Dodson AH, Liu J (2009) Ambiguity resolution in precise point positioning with hourly data. GPS Solut 13(4):263–270

Geng J, Meng X, Dodson AH, Teferle FN (2010) Integer ambiguity resolution in precise point positioning: method comparison. J Geod 84(9):569–581

Geng J, Teferle FN, Meng X, Dodson AH (2011) Towards PPP-RTK: ambiguity resolution in real-time precise point positioning. Adv Sp Res 47(10):1664–1673

Gu SF, Lou YD, Shi C, Liu JN (2015) BeiDou phase bias estimation and its application in precise point positioning with triple-frequency observable. J Geod. doi:10.1007/s00190-015-0827-z

Griffiths J, Ray J (2009) On the precision and accuracy of IGS orbits. J Geod 83(3):277–287

Guo F, Zhang XH, Wang JL (2015) Timing group delay and differential code bias corrections for BeiDou positioning. J Geod 89(5):427–445

Huber K, Hinterberger F, Lesjak R, Weber R (2014) Real-time PPP with ambiguity resolution—determination and application of uncalibrated phase delays. In Proceedings of the ION GNSS, Tampa, FL, USA, 8–12 Sept 2014, pp 976–985

Ji S, Chen W, Ding X, Chen Y, Zhao C, Hu C (2010) Ambiguity validation with combined ratio test and ellipsoidal integer aperture estimator. J Geod 84(10):597–604

Jokinen A, Feng S, Milner C, Schuster W, Ochieng W (2011) Precise point positioning and integrity monitoring with GPS and GLONASS. In: European navigation conference 2011

Jokinen A, Feng S, Schuster W, Ochieng W, Hide C, Moore T, Hill C (2013) GLONASS aided GPS ambiguity fixed precise point positioning. J Navig 66(3):399–416

Kouba J, Héroux P (2001) Precise point positioning using IGS orbits and clock products. GPS Solut 5(2):12–28

Laurichesse D, Mercier F, Berthias JP, Broca P, Cerri L (2009) Integer ambiguity resolution on undifferenced GPS phase measurements and its application to PPP and satellite precise orbit determination. Navigation 56(2):135–149

Li P, Zhang XH (2014) Integrating GPS and GLONASS to accelerate convergence and initialization times of precise point positioning. GPS Solut 18(3):461–471

Li P, Zhang XH (2015) Precise point positioning with partial ambiguity fixing. Sensors 15(6):13627–13643

Li X, Ge M, Zhang H, Wickert J (2013) A method for improving uncalibrated phase delay estimation and ambiguity-fixing in real-time precise point positioning. J Geod 87:405–416

Li M, Qu LZ, Zhao QL, Guo J, Su X, Li XT (2014) Precise point positioning with the BeiDou navigation satellite system. Sensors 14(1):927–943

Li P, Zhang XH, Ren XD, Zuo X, Pan YM (2015a) Generating GPS satellite fractional cycle bias for ambiguity-fixed precise point positioning. GPS Solut 1–12. doi:10.1007/s10291-015-0483-z

Li X, Ge M, Dai X, Ren X, Fritsche M, Wickert J, Schuh H (2015b) Accuracy and reliability of multi-GNSS real-time precise positioning: GPS, GLONASS, BeiDou, and Galileo. J Geod 89:607–635

Lou Y, Liu Y, Shi C, Yao XG, Zheng F (2014) Precise orbit determination of BeiDou constellation based on BETS and MGEX network. Sci Rep 4:4692

Loyer S, Perosanz F, Mercier F, Capdeville H, Marty J (2012) Zero-difference GPS ambiguity resolution at CNES-CLS IGS Analysis Center. J Geod 86(11):991–1003

Melbourne WG (1985) The case for ranging in GPS-based geodetic systems. In: Proceedings of the first international symposium on precise positioning with the global positioning system, Rockville, 15–19 April, pp 373–386

Pan L, Cai C, Santerre R, Zhu J (2014) Combined GPS/GLONASS precise point positioning with fixed GPS ambiguities. Sensors 14(9):17530–17547

Petit G, Luzum B (2010) IERS Technical Note No. 36, IERS Conventions 2010, International Earth Rotation and Reference Systems Service, Frankfurt, Germany

Qu LZ, Zhao QL, Guo J, Wang GX, Guo XX, Zhang Q, Jiang KC, Luo L (2015) BDS/GNSS real-time kinematic precise point positioning with un-differenced ambiguity resolution. In: Sun J, Jiao W, Wu H, Lu M (eds) China satellite navigation conference (CSNC) 2015 Proceedings, vol II. Springer, Berlin, Heidelberg, pp 13–29

Reussner N, Wanninger L (2011) GLONASS Inter-frequency biases and their effects on RTK and PPP carrier phase ambiguity resolution. In: Proceedings ION-GNSS-2011, Institute of Navigation, Portland, OR, pp 712–716

Saastamoinen J (1972) Atmospheric correction for troposphere and stratosphere in radio ranging of satellites. In: Henriksen S, Mancini A, Chovitz B (eds) The use of artificial satellites for geodesy, vol 15. Geophysics monograph series. AGU, Washington DC, pp 247–251

Schmid R, Rothacher M, Thaller D, Steigenberger P (2005) Absolute phase center corrections of satellite and receiver antennas. GPS Solut 9(4):283–293

Schmid R, Steigenberger P, Gendt G, Ge M, Rothacher M (2007) Generation of a consistent absolute phase-center correction model for gps receiver and satellite antennas. J Geod 81(12):781–798

Shi J, Gao Y (September 2012) A fast integer ambiguity resolution method for PPP. In Proceedings of the ION GNSS, Nashville, TN, USA, vol 17–21, pp 3728–3734

Sleewaegen JM, Simsky A, de Wilde W, Boon F, Willems T (2012) Demystifying GLONASS inter-frequency carrier phase biases. Inside GNSS 7(3):57–61

Steigenberger P, Montenbruck O, Weber R, Hugentobler U (2013) Status and perspective of the IGS multi-GNSS experiment (MGEX). In: EGU general assembly conference abstracts, vol 15, p 2558

Takasu T, Yasuda A (2010) Kalman-filter-based integer ambiguity resolution strategy for long-baseline RTK with ionosphere and troposphere estimation. In: Proceedings of the ION GNSS, Portland, OR, USA, 21–24 Sept 2010, pp 161–171

Teunissen PJG (1995) The least-squares ambiguity decorrelation adjustment a method for fast GPS integer ambiguity estimation. J Geod 70(1–2):65–82

Teunissen PJG, Joosten P, Tiberius C (1999) Geometry-free ambiguity success rates in case of partial fixing. In: Proceedings of ION NTM, San Diego, CA, USA, 25–27 Jan 1999, pp 201–207

Teunissen PJG, Odolinski R, Odijk D (2014) Instantaneous BeiDou + GPS RTK positioning with high cut-off elevation angles. J Geod 88(4):335–350

Verhagen S, Teunissen PJG, van der Marel H, Li B (2011) GNSS ambiguity resolution: which subset to fix? In: Proceedings of the 2011 IGNSS symposium, International Global Navigation Satellite Systems Society, Sydney, Australia, 15–17 November 2011; pp 1–15

Wang J, Feng Y (2013) Reliability of partial ambiguity fixing with multiple GNSS constellations. J Geod 87(1):1–14

Wanninger L, Beer S (2015) BeiDou satellite-induced code pseudorange variations: diagnosis and therapy. GPS Solut 19(4):639–648

Wu JT, Wu SC, Hajj GA, Bertiger WI, Lichten SM (1993) Effects of antenna orientation on GPS carrier phase. Manuscripta Geodaetica 18(2):91–98

Wubbena G (1985) Software developments for geodetic positioning with GPS using TI-4100 code and carrier measurements. In: Proceedings of first international symposium on precise positioning with the global positioning system, Rockville, 15–19 April, pp 403–412

Zhang XH, Li P (2013) Assessment of correct fixing rate for precise point positioning ambiguity resolution on global scale. J Geod 87(6):579–589

Zhao Q, Guo J, Li M, Qu L, Hu Z, Shi C, Liu J (2013) Initial results of precise orbit and clock determination for COMPASS navigation satellite system. J Geod 87(5):475–486

Zumberge JF, Heflin MB, Jefferson DC, Watkins MM, Webb FH (1997) Precise point positioning for the efficient and robust analysis of GPS data from large networks. J Geophy Res 102(B3):5005–5017